Investigation of Beam- and Wave- Plasma Interaction in the Globus-M Spherical Tokamak

V.K. Gusev 1), S.E. Aleksandrov 1), R.M. Aminov 2), A.G. Barsukov 3), A.A Berezutskiy 1), V.V. Bulanin 4), F.V. Chernyshev 1), I.N. Chugunov 1), A.V. Dech 1), V.V. Dyachenko 1), A.E. Ivanov 1), S.A. Khitrov 1), N.A. Khromov 1), M.M. Kochergin 1), S.V. Kobyakov 4), G.S. Kurskiev 1), E.A. Kuznetsov 5), V.M. Leonov 3), M.M. Larionov 1), A.D. Melnik 1), V B. Minaev 1), A.B. Mineev 6), M.I. Mironov 1), I.V. Miroshnikov 4), E.E. Mukhin 1), A.N. Novokhatsky 1), A.A. Panasenkov 3), M.I. Patrov 1), A.V. Petrov 4), M.P. Petrov 1), Yu.V. Petrov 1), K.A. Podushnikova 1), V.A. Rozhansky 4), V.V. Rozhdestvensky 1), N.V. Sakharov 1), A.E. Shevelev 1), I.Yu. Senichenkov 4), O.N. Shcherbinin 1), A.Yu. Stepanov 1), G.N. Tilinin 3), S.Yu. Tolstyakov 1), V.I. Varfolomeev 1), A.V. Voronin 1), V.A. Yagnov 5), A.Yu. Yashin 4), E.G. Zhilin 7)

1) Ioffe Physical-Technical Institute of the Russian Academy of Sciences, St.Petersburg, Russia
2) St. Petersburg State University, St.Petersburg, Russia
3) Institute of Tokamak Physics RRC "Kurchatov Institute", Moscow, Russia
4) Saint Petersburg State Polytechnical University, St.Petersburg, Russia
5) State Research Center of Russian Federation, TRINITI, Moscow region, Troitsk, Russia
6) D.V.Efremov Institute of Electrophysical Apparatus, St.Petersburg, Russia
7) Ioffe Fusion Technology Ltd., St.Petersburg, Russia

e-mail contact of main author: vasily.gusev@mail.ioffe.ru

Abstract. Experimental and theoretical results on interaction of neutral particle beams and HF waves with plasma obtained during last two years on the spherical tokamak Globus-M are discussed in the report. It is shown that high density (up to 3×10^{22} m^{-3}) and high velocity (up to 250 km/s) plasma jet injection (which is analogous to the injection of low energy neutral beam) may produce a moderate density rise (up to 30%) in the central plasma region without plasma disruption. The confinement of fast particles with mainly parallel velocities during high energy neutral beam injection (NBI) is discussed. The data on fast particle losses and influence on the magnetic field on their confinement are argued. New results on the heating of ions and electrons in Globus-M are shown. EPM in the range of 5-30 kHz and TAE modes in the range of 50-300 kHz were recorded with NBI shots, in which fast ion velocity exceeds Alfven velocity. EPM and TAE mode amplitudes $\tilde{B}/B_t$ were: ~ 5×10^{-3} and ~ 2×10^{-4} correspondingly. EPM and TAE modes demonstrated the significant difference from NSTX mode behavior. On Globus-M the TAE spectrum looks like narrow band, corresponding to n=1. The first results of the experiment on plasma start-up and noninductive CD generation by means of waves with frequency higher than lower hybrid one (920 MHz) are discussed. Experimental conditions are described. High CD efficiency is shown (about 0.25 A/W), CD mechanism is proposed. Near future plans of experiments are discussed. It is proposed to improve the efficiency of utilized heating methods by the increase of the magnetic field.

1. Introduction`

The range of investigations was performed on Globus-M since last FEC IAEA conference [1-8]. Novel results were obtained in the field of NB injection experimental study and modeling. Energetic particle modes (EPM) and Alfven eigenmodes study was started. For the first time experiments on plasma start-up and noninductive CD generation were performed in the range of frequency few times higher than LH one.

The current report is devoted to the overview of the results, joint by the physics of interaction of beams, particles and HF waves with spherical tokamak plasmas in the Globus-M.

2. Injection of low energy beam by a plasma gun

The hydrogen plasma gun, generating the plasma jet of high velocity and density and short duration is utilized on Globus-M. Due to high density the beam recombines to become a beam

of low energy neutrals during time of plasma jet flight to plasma [9]. Improved gun modification used in last time experiments could produce plasma jet with kinetic energy up to
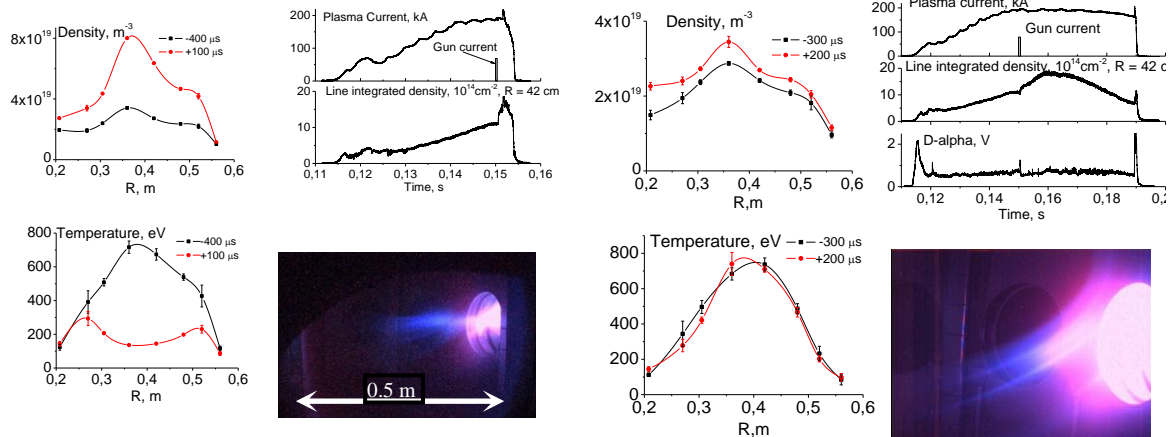

FIG. 1. Penetration of higher energy jet into the plasma column; shot 26900; accelerating voltage is 4.4 kV

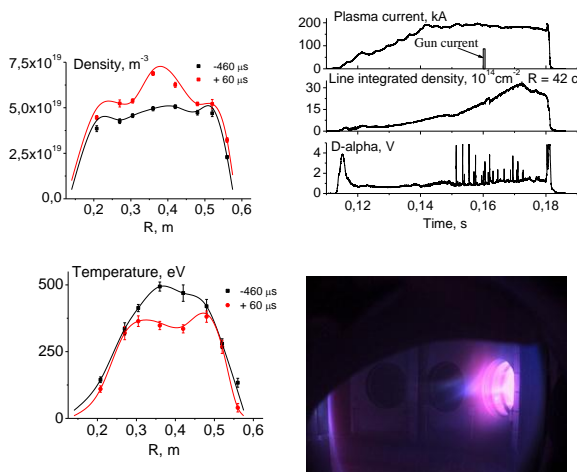FIG.2. Penetration of lower energy jet into the plasma column; shot 26836; accelerating voltage is 4.2 kV

FIG.3. Jet penetration into the plasma column after H-mode initiation with NBI; shot 26896; accelerating voltage 4.4 kV

300 eV [2]. Jet density was increased up to 3×10^{22} m^{-3}. Jet (beam) particles could penetrate deep into the plasma core and beyond due to high velocity up to 250 km/s. Beam particles are promptly ionized inside plasma and produce fast density rise. Beam-plasma interaction dynamics was analyzed with the help of upgraded Thomson scattering (TS) system [4]. The fast video camera and the streak-camera diagnostic set were also used. The profiles of electron temperature and density, picked up before (-400 and -300 μs) and shortly after injection (100 and 200 μs), the traces of plasma current and density variation, as well as video frame of beam trace inside plasma are shown in fig. 1 and 2. Figure 1 shows the strong penetration of the beam into the plasma column (probably throughout the column). Density rises more than 3 times and temperature drops over the whole column which results in plasma disruption in a few ms interval. Decrease of accelerating voltage (fig. 2) lowers the beam energy and as a result one could see only 20% density increase. The discharge accepts it easily and does not disrupt. Even more, the transition to the H-mode regime occurred due to injection. Injection into the stationary H-mode phase was also performed. One could see from fig. 3 as the "table-like" density profile, typical for such stage of a discharge gets a "hat" in the central part shortly after injection. The

FIG.4. The video-frames of the jet injected in the target plasma with superimposed simulated fragments of the magnetic field lines.

central core density rise is accompanied by the small temperature drop in the core. Other discharge parameters do not change. Beam particles which are protons after ionization inside the plasma column are tightly bond to the field lines. Recombination of protons moving along the magnetic field makes the field lines visible. It looks like highlighting of the field line in the region of beam penetration and braking. Which boundary or core magnetic field lines are highlighted is dependent on beam energy. Unfortunately, until now we could not reliably and predictably change the beam
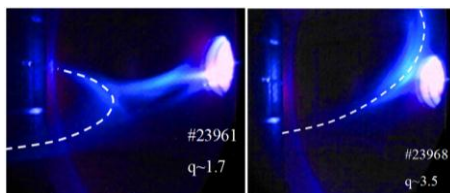
energy and effect is statistically non reproducible. Nevertheless this effect gives the principal opportunity to study safety factor distribution (q profile) visually. Corresponding pictures are shown in fig.4.

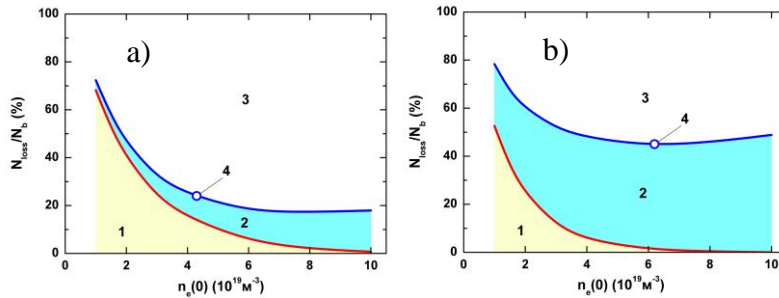## 3 Neutral beam injection and fast particle behavior

FIG. 5. Relative number of fast particles lost by: 1-shine through, 2- from first orbit. 3- confined particles. Simulations made for the density marked 4, $E_b = 18$ keV, hydrogen beam – a, deuterium –b. Plasma configuration as in shots 21407, 21473 correspondingly.
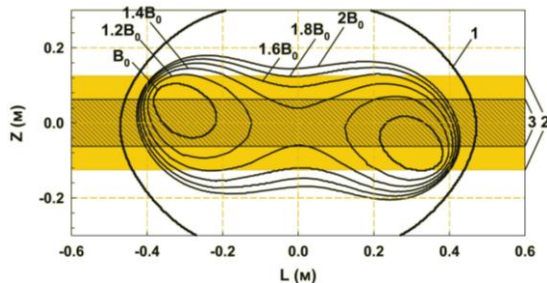
FIG. 6. Vertical slice of plasma column passed along the beam axis. Fast particles are confined inside zones marked by B_0, $1,2B_0$, etc., where $B_0=0.4$ T 1-plasma boundary, 2-beam full width (FW), 3-beam FWHM. Plasma configuration as in shot 21407
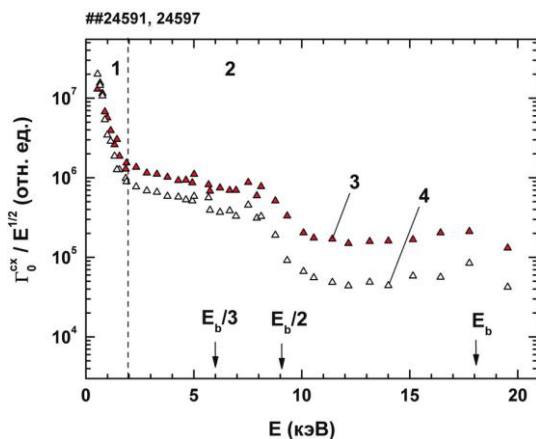

FIG.7. Charge exchange hydrogen atom spectra recorded by NPA ACORD-M. Tangential line of sight. $E_b=18$ кэВ. E_b, $E_b/2$, $E_b/3$ – beam energy components. 1-thermal energy range, 2-suprathermal energy range, 3 - B=0.4 T, 4 – B=0.33 T

Significant part of the neutral beam power is not transferred to the plasma particles and lost during NB injection in Globus-M [10]. So called "direct" losses, i.e. shine-through and first orbit losses, play the main role. First orbit losses are the most crucial for spherical tokamaks due to relatively weak magnetic field and, hence, essential deviation of fast ion orbits from magnetic surfaces. Special 3D numerical code was developed to simulate particle "direct" losses [11]. It includes beam particle ionization and fast ion trajectory calculations. Code utilizes magnetic field map reconstructed by EFIT [12]. The simulated dependence of "direct" fast ion losses from Globus-M versus plasma density is shown in fig. 5 for hydrogen and deuterium beam injection with the particle energy of 18 keV.The "direct" losses could reach 70-80% at the low density ($n_e(0) \sim 1 \times 10^{19}\,\text{m}^{-3}$) and decrease with density rise, as it follows from simulation results. It is worth noting that shine-through losses are higher for the hydrogen beam (about half for the density $5 \times 10^{19}\,\text{m}^{-3}$). First orbit losses are higher for deuterium beam and full particle number lost "directly" is higher for deuterium beam also. The increase of beam energy enhances the direct losses even at high plasma density [13]. However, fast particle orbit losses could be suppressed significantly by the increase of toroidal field. Figure 6 shows the vertical slice of fast particle confinement zones, simulated for the deuterium beam of 30 keV energy injected into the plasmas with several toroidal magnetic field values in the range of 0.4-0.8 T. To keep the magnetic configuration unchanged the corresponding variation of plasma current was applied in simulations. The zone of confined particles at standard magnetic field (marked B_0) is represented by two small area islands placed at the entrance and exit of the beam to/from the plasma. At the increased toroidal field the zone area enlarges also and fully overlaps the beam trajectory when the magnetic field doubles,

B_0=0.8 T. Thus even the moderate toroidal field increase could lead to the significant decrease of the fast particle losses from the Globus-M plasma. E.g. to decrease the particle losses down to 20% it is enough to increase the magnetic field strength (poloidal+toroidal) by 40% at the plasma density $n_e(0) \sim 6 \times 10^{19}$ m^{-3}.
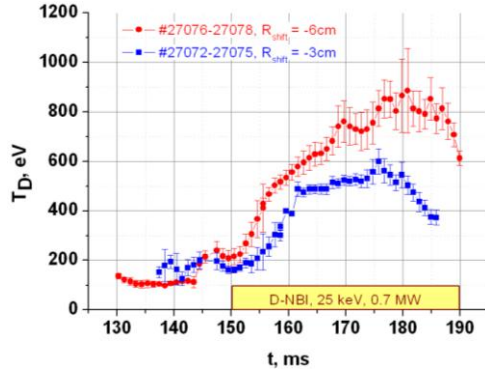
FIG. 8. Ion temperature measured by NPA ACORD-12. Normal line of sight. Red – shifted and blue – non shifted plasma column

Experimental verification of numerical simulations was made in experiments with a reduced magnetic field [3]. The injection of 18 keV hydrogen beam was performed in two regimes with $B_t = 0.41$ T and $B_t = 0.33$ T ($I_p = 205$ and 165 кА). The simulations predict the enhancement of fast particle losses at such conditions. Figure 7 shows the fast particles spectra picked up by the NPA tangentially directed to the magnetic axis of the plasma column. The NPA tangential angle was equal to the beam injection angle. The spectra were measured at 15 ms after NB start. One could see from the spectra that particle fluxes recorded at 0.33 T are significantly lower than corresponding fluxes at 0.41 T. The largest diffe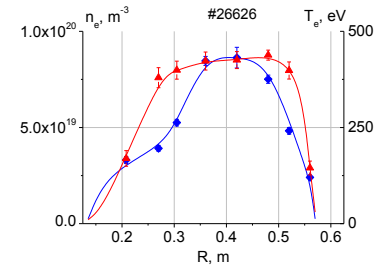rence of the fluxes observed in the energy range of $E_b/2$ – E_b, testifies the increase of full energy fast particle losses. The detailed analysis shows that full energy particle losses at the lower field increase from 25 to 40%, which is slightly higher than simulation predictions (from 24 to 32%). The main result of such experiments and simulations is a strong dependence of the fast particle confinement on the magnetic field value. In spite of the big losses of fast particles, NB heating helped to improve plasma parameters achieved at the Globus-M tokamak. During injection of 25 keV deuterium beam into the low density plasma with the column shifted slightly inward (- 3cm from the standard position) the ion temperature reaches 0.85 keV at 0.7 MW injection power (see fig. 8) [3].

Electron heating in Globus-M was discussed before [9]. The heating conditions are challenging in low magnetic field small spherical tokamaks due to unfavorable ratio of the energy confinement time to the beam slowing down time [10]. In spite of this, regimes in which electron heating is more effective exist. Promising results were obtained in the shots with the high current ramp up speed (8.5 MA/s) and the early beam injection time (7 ms after start-up). Figure 9 shows comparison of electron temperature and density profiles. As it is seen from the figure, the temperature profile is evidently wider than the density one. This may be a result of unusual for Globus-M confinement improvement. Usual H-mode resulted in the wide density and more narrow temperature profiles. The transport modeling is on the way.

FIG.9. Electron temperature (red) and density(blue) profiles in shot 26626 (early beam injection, fast current ramp-up). P_{beam}=0.8 MW, E_{beam}=27 keV. The profiles measures at 26 ms after NB start at the current plateau (146 ms)

4. Energetic particle modes and Alfven eigenmodes

Under neutral beam injection into Globus-M, a wide variety of fast ion driven instabilities may be excited due to the large ratio of fast ion velocity to Alfven velocity V_f/V_A, that can reach the value of 3 [15]. Two branches of fast ion driven instabilities are observed in the experiment: the low frequency energetic particle mode (EPM), in the range of 5-30 kHz, and the high frequency Alfven eigenmodes (AE), in the range of 50-300 kHz. The low frequency fluctuations with an amplitude relative to the toroidal field ($\tilde{B}/B_t$) up to 5×10^{-3} are observed with the usual Mirnov probe. The amplitude of high frequency fluctuations is much lower, ($\tilde{B}/B_t$) $\sim 2 \times 10^{-4}$, therefore they are observed with Alfven loop of 200 см^2 area, placed in the equatorial plane inside the vacuum vessel and equipped by a band amplifier with maximum amplification in the range of 100-200 kHz. EPM are observed in different tokamak operation

regimes and mostly represent usual fishbone modes. Up to the last time we could not record AE on Globus-M. For the first time we managed to detect them in shots with early

NBI. At that, a flat profile of the plasma current density remain in an initial stage of the discharge, the central q did not drop lower than 1, and sawtooth were absent. AE disappeared with the sawtooth beginning. The recorded modes were identified as toroidal AE (TAE) due to their frequency range and behavior features. The modes demonstrate correct tendency of the frequency on density (i.e. on the Alfven velocity) both during one shot (decreasing of the frequency as the density increase), and in the shots with different beams (deuterium and hydrogen). A different behavior pattern was observed. Mostly, the mode arose in the form of single or periodic bursts of 1 ms duration with the growth time of several hundred microseconds. Under favorable conditions a regular burst lasted up to several ms at approximately constant amplitude. Waveforms of shot #27498 are presented in fig. 10, which show that the TAE exists until $q(0)$ does not drop to 1 and sawtooth does not appear. During one burst the TAE frequency can change smoothly or exhibit chirping. The typical spectrograms for the two cases (shots #27498 and #27328) are presented in fig. 11.
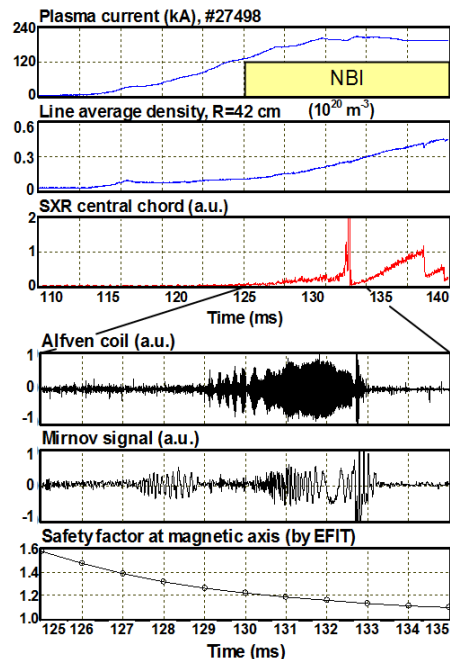

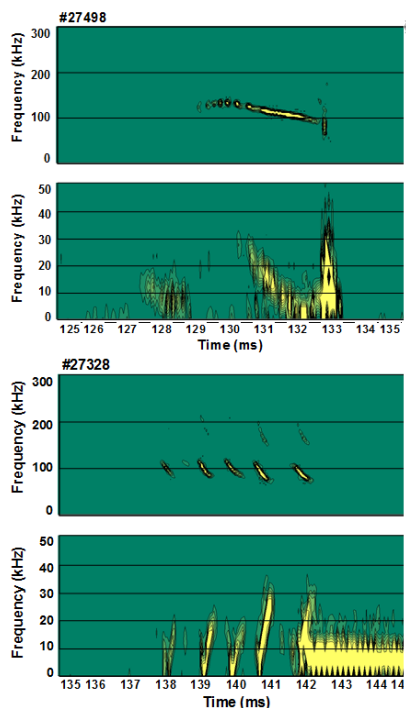*FIG. 10. Plasma parameter waveforms in shot 27498*

FIG. 11. Spectrograms, showing TAE and EPM activity in shots with fast (27498) and slow (27328) plasma current ramp up

The fast ion driven mode behavior on Globus-M demonstrates both some similar characteristics with analogous modes observed on NSTX and MAST spherical tokamaks, and a row of peculiarities. Although the bursts of the EPM arose synchronously with TAE, they reveal the absolutely different temporal behavior. As it is seen from fig.11 (shot #27328), the EPM frequency during the burst first sharply drops, then increases, while the TAE frequency monotonously drops. Unlike experiments on NSTX [17], forming of the toroidally localized TAE wave packet in a fixed position with respect to EPM perturbation did not occur. The both modes exist like independent ones. Another peculiarity concerns the TAE. In the perturbation spectrum, as a rule, only one mode of toroidal number $n=1$ exists, in contrast to the situation on NSTX [18], where several modes at once with $n=1$-7 were observed. Perhaps it is explained by different experimental conditions on Globus-M, where relation V_f/V_A was near 1.4, unlike on NSTX, where it was much higher.

If we use the estimation formula for the mode frequency from [15]: $\omega_{TAE}=V_A/2qR$, then, substituting to this relation the values of frequency and density from the experiment, we obtain for the deuterium and hydrogen beams $qR=1$ and 1.1 respectively. Only $q=2$, $R=0.5$ satisfy this relation. Actually, the EFIT code gives $r=15$ cm (i.e. $R \approx 0.5$ m) for the surface $q=2$. One can suppose that the instability develops near the surface $q=2$, on the outer region. Then the estimates of the most unstable mode number by means of formulas from paper [19] give $n \approx 1$. Thus, in the experimental conditions of Globus-M, perturbations with $n=1$ have to develop predominantly. That is confirmed by the Fourier spectrum of

distortion, in which only single rather narrow line for the first harmonic and essentially weaker second harmonic exists (see fig. 11). In the carried out experiments, the great number of peaks corresponding to different values of n (as it was in the NSTX experiments) were not recorded.

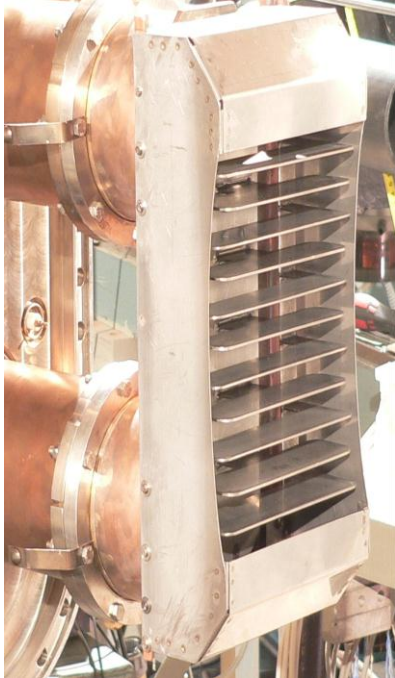## 5. Lower hybrid non inductive plasma start-up and current drive

FIG.12.RF antenna for CD experiments

A new approach for solving the CD problem in spherical tokamaks is investigated on Globus-M. Conception of LHCD experiments, its theory and numerical simulation at 2.45 GHz frequency were presented in [20-22]. The preliminary experiments at lower frequency 900 MHz and power $P<60$ kW have been started. The wave excitation was performed by a comb-like antenna oriented in poloidal direction which is shown in fig.12. The horizontal plates of the antenna were connected alternatively to the grounded strap or to the current strap. HF fields between the plates are directed vertically, imitating the work of a waveguide grill. But unlike the grill the strong horizontal fields arise between the plates and grounded screen. Considering the antenna geometrical dimensions and the vacuum wave length (30 cm) one can expect in radiated spectrum $N_{tor} \approx (1.0-15)$ − for toroidally slowed waves and $N_{pol} \approx (7-8)$ − for poloidal slowing down. The symmetrical spectrum is expected both in co and counter magnetic field direction.The experiments were carried out at B_t=0.4 T [23]. In discharge scenario the toroidal field and small vertical field $B_v \cong$2.0-2.5 mT were applied before the RF pulse. The value of B_V at the breakdown stage was taken to obtain maximal current ramp-up rate at the discharge start.

It should be noted that the initial current arose at the stationary phase of B_v , when the induced electric field was absent completely, $U_{loop} = - d\Phi_v/ dt$ =0. The plasma parameter traces during the RF pulse, input RF power, driven current, MHD, line-averaged density, vertical magnetic field, D_α , HXR radiation, 17 GHz radiation are shown in fig.13. One can distinguish three stages of the discharge formation. At the RF start (3-4 ms) the ionization takes place (see peak in D_α), and the plasma fills up the volume of the torus. The fast video camera shows it distinctly. After 3-5 ms, the toroidal current reaches 4-5 kA with the rate 450-500 kA/s, which is comparable with traditional experiments on LHCD in tokamaks. The current direction was dependent on the direction of B_V. At the next stage of the discharge, the vertical magnetic field should be enhanced to increase the plasma current. The rate of current ramp-up is about 200 kA/s. Too fast increase leads to the discharge disruption. At achieving the optimal level the
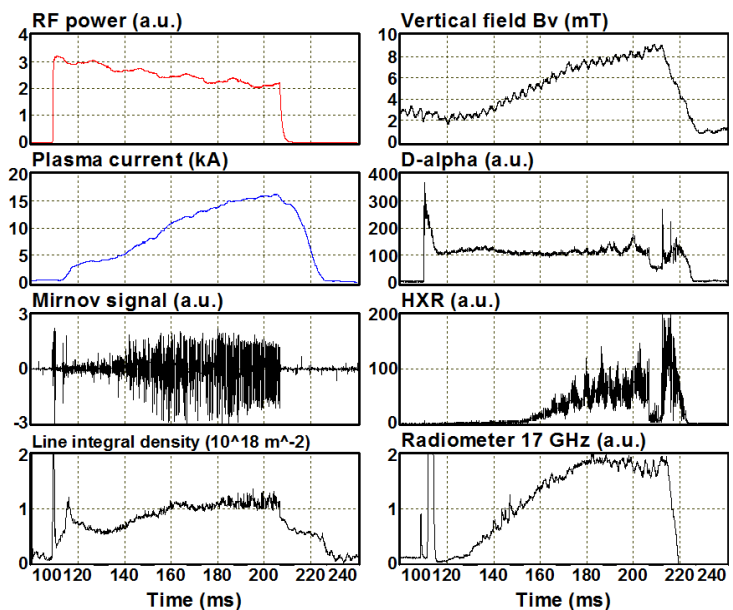

FIG.13. Plasma parameters waveforms in CD experiment, shot 26715

current ceased to increase and passed into saturation phase. In the best shots the current

amplitude achieved 15-17 kA at plasma density $(1-2) \times 10^{18}$ m^{-3}. The electron temperature measured by TS reaches 15-20 eV. The driven current lasted during the whole HF pulse (100 ms) and depended weakly on HF power in the range 20–40 kW. No signals were registered at the loop voltage control except inductive spikes at the beginning and at the end of the current. The current ramp-up was accompanied by increase of synchrotron and HXR radiation, which evidenced the formation of high energy electrons. The synchrotron radiation was observed in a broad frequency range − 12-36 GHz with small delay after the current start. The radiation temperature can be evaluated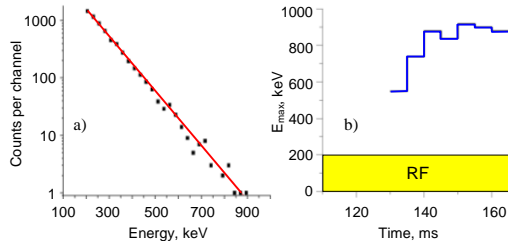 as several keV. The HXR radiation was analyzed by a spectrometer starting from the energy 0.2 MeV. HXR spectrum averaged on a few discharges is shown in fig.14a. It lasted up to $E_{\mathrm{Max}} \approx 0.9$ MeV. This value can be taken as the upper limit of the electron energy. Figure 14b shows the delay of maximal HXR energy counts ($E_{\mathrm{Max}} \geq 550$ keV) from the current start up at 110 ms. Probably the fast electrons need time to achieve high energies during acceleration. The delay also testifies the good confinement of electrons at the first stage.

FIG. 14 HXR spectrum (a) and maximal gamma photon energy temporal evolution (b)

Interestingly that CX diagnostics observes the "tails" of high energy ions in these "cold" discharges. Figure 15 shows the energy spectra of ions for time interval 163±1.5 ms. The spectrum lasts up to 1.5 keV energy, and "effective" temperature is about 200-300 eV. The appearance of such ions due to collisions with the fast electrons is practically impossible. The mechanism of their generation is unknown yet.

The spectral analysis of HF plasma radiation reveals the appearance of satellites of pumping frequency shifted in low frequency side on several ion cyclotron harmonics. One can assume that described above the fast ion "tails" in the energy spectra can appear at absorption of these harmonics in resonance condition. Essential increase of radiation with fine frequency structure was observed also in 400-500 MHz frequency range. It manifests the development of non-linear decay processes, which in turn could be an additional mechanism of fast electron generation. Parametric decay instabilities take place in the current ramp-up stage only and vanishe in the stationary phase at maximal currents.

The probable scenario of the discharge development looks like that: the electric HF fields on the antenna surface produce two groups of fast electrons moving co and counter the toroidal field. The vertical field B_v saves only one of them, shifting it inside, when the other one perishes on the wall. Remained electrons interact with slowed down waves and gain higher energy, sustaining plasma current. The parametric decay processes enhance the current rise.
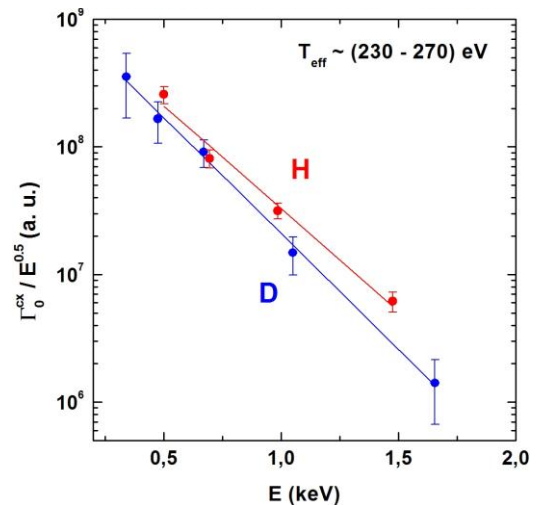

FIG. 15. Charge exchange atom spectra in the shot 26280 with CD

6. Discussion, future plans and summary

Influence of beams and HF waves on the Globus-M plasma is more diverse than follows from results described above. Big attention is paid to the study at L and H regimes obtained during the interaction of beam and wave with plasma. Diagnostics instrumentation used in the experiment permit to investigate details of such processes. In addition to upgraded multipulse TS diagnostics already mentioned above, the new Doppler reflectometer is commissioned. The first results on plasma rotation and filament structure near the edge are obtained in the L and H modes [24].

Integral modeling of the Globus-M plasma is on the way. The efforts are performed with the help of numerical codes ASTRA (1D modeling of central plasma region) and B2SOLPS5.2 code (2D plasma edge and SOL). New effects were recorded after Alfven instability diagnostic set was commissioned. TAE spectrum in Globus-M is recorded and found limited to the basic harmonic, n=1. Efforts on the diagnostics resolution improvement are performed to allow the study of fast particle instabilities influence on the D-D beam-plasma reaction rate. Plasma start-up and noninductive CD experiments were conducted in the frequency range 920MHz, which is several times higher than LH one with the simplified antenna model. The effective CD generation is demonstrated. The full scale CD experiment is under preparation, the multi-junction grill, RF equipment, including a klystron generator are partly manufactured. The latest results by the full wave code simulation at 2.45 GHz frequency predict significant CD in the Globus-M plasma [25]. The nearest experimental plans also include the basic harmonic ICRH experiments, which have already demonstrated good heating efficiency [1]. A new designed double loop antenna is under manufacturing now. Novel simulations of trajectories for the fast particles generated during ICRH with perpendicular velocity vector were performed [6]. Simulations predict significant increase in the energy of confined particles (up to 1.5 times) at a moderate toroidal magnetic field increase (20%).The results of simulations and experiments predict the radical decrease of the fast particle losses at the toroidal magnetic field rise. The NB absorption and antennae-plasma coupling are expected to improve. Taking into account confinement improvement, the synergetic effect of toroidal magnetic field increase is supposed. Currently the design of a novel Globus-M central column is started. The column permits 1.5 toroidal field increases.

References
[1] GUSEV V.K., et al., Nuclear Fusion, **49** (2009) #104021
[2] VORONIN A.V., et al., Proc. of 37th EPS PPC, Dublin, 2010, P5.192
[3] MINAEV V.B., et al., Proc. of 37th EPS PPC, Dublin, 2010, P5.192
[4] TOLSTYAKOV S.Yu., et al., Proc. of 37th EPS PPC, Dublin, 2010, P5.137
[5] PETROV Yu.V., et al., Plasma Physics Reports, **36** (2010) 455
[6] CHERNYSHEV F.V., et al., Plasma Physics Reports, **35** (2009) 903
[7] SENICHENKOV I.Yu., ROHZANSKY V.A.,19th Culham-Ioffe Symp., St.Petersburg, 2010
[8] GUSEV V.K., et al., Proc. of 37th EPS PPC, Dublin, 2010, P2.167
[9] GUSEV V.K., et al., Nucl. Fusion, **46** (2006) S584
[10] AYUSHIN B.B., et al., Plasma Physics Reports, **34** (2008) 81
[11] CHERNYSHEV F.V., et al., Plasma Physics Reports, **37** (2011) *to be published*
[12] LAO L.L., et al., Nuclear Fusion, **25** (1985) 1611
[13] PATROV M.I., et al., Proc. 36th EPS PPC, Sofia, 2009, ECA vol. 33E, P-5.153
[14] MINAEV V.B., et al., Proc. 35th EPS PPC, Hersonissos, 2008, ECA vol. 32D, P-1.110
[15] ITER Physics Basis, Nucl. Fusion, **12** (1999) 2478
[16] FREDRICKSON E.D., et al., Physics of Plasmas, **10** (2003) 2852
[17] FREDRICKSON E.D., et al., Phys. Rev. Letters **97** (2006) 045002
[18] FREDRICKSON E.D., et al., Physics of Plasmas **13** (2006) 056109
[19] GORELENKOV N.N., et al., Physics of Plasmas **11** (2004) 2586
[20] GUSEV V.K., et al., Tech.Phys., **44** (1999) 1054
[21] IRZAK M.A., 30th EPS CF&PPC, St.Petersburg, 2003, ECA vol. 27A, P-2.175
[22] SHCHERBININ O.N., et al., 18th Top. Conf. on RF Power in Plasmas, Gent, 2009, AIP Conf. Proc., **1187**, 427
[23] DYACHENKO V.V., et al., Proc. 37th EPS PPC, Dublin, 2010, P5.151
[24] BULANIN V.V., et al., Proc. 37th EPS PPC, Dublin, 2010, P1.1012
[25] GUSAKOV E.Z., et al., Plasma Phys. Control. Fusion **52** (2010) 075018